American Mineralogist, Volume 86, pages 997–1002, 2001

# Phase relations of $CaCO_3$ at high pressure and high temperature

KAICHI SUITO,[1,*] JUNPEI NAMBA,[1] TAKASHI HORIKAWA,[1] YOZO TANIGUCHI,[1] NORIKO SAKURAI,[1]
MICHIHIRO KOBAYASHI,[1] AKIFUMI ONODERA,[1] OSAMU SHIMOMURA,[2] AND TAKUMI KIKEGAWA[3]

[1]Graduate School of Engineering Science, Osaka University, Toyonaka, Osaka 560-8531, Japan
[2]SPring-8, Japan Atomic Energy Research Institute, Sayo, Hyogo 679-5198, Japan
[3]Photon Factory, Institute of Materials Structure Science, High Energy Accelerator Organization, Tsukuba, Ibaraki 305-0801, Japan

## ABSTRACT

Phase transitions in calcite, a naturally occurring crystalline form of $CaCO_3$, have been investigated by three different experimental techniques: (1) in-situ X-ray diffraction (XRD) using synchrotron radiation to 6 GPa and 1750 °C in a cubic anvil press; (2) Raman scattering to 10 GPa at room temperature using a diamond-anvil cell; and (3) post-compression XRD on samples retrieved after heat treatment at temperatures to 2000 °C and pressures to 9 GPa in an octahedral anvil press. At room temperature, calcite I transformed into calcite II at 1.7 GPa and then to calcite III at ~2 GPa. Calcite III persisted to at least 10 GPa. Elevation of temperature at 3, 4, and 6 GPa caused a sequence of transitions: calcite III $\rightarrow$ aragonite $\rightarrow$ disordered calcite $\rightarrow$ liquid, and aragonite was retained upon rapid cooling of the liquid. The melting curve of disordered calcite increased with pressure following a relation: $T_m$ (°C) = 1338 + 82 $P$ – 2.9 $P^2$ where $P$ is in units of GPa.

## INTRODUCTION

In nature, calcium carbonate ($CaCO_3$) occurs in three structural forms: rhombohedral calcite, orthorhombic aragonite, and hexagonal vaterite. Calcite is stable at atmospheric pressure, whereas aragonite is thermodynamically stable under pressure but can be retained to ambient conditions. The stability field of vaterite is not well established.

Various laboratory experiments have revealed that calcite exists in five different modifications (calcite I, II, III, IV, and V) over ranges of pressure and temperature (Mirwald 1976; Liu and Bassett 1986). (For clarification we will refer to ordinary rhombohedral calcite as calcite I in this paper.) The first finding of the high-pressure phases of calcite (calcite II and III) by Bridgman (1938) using volumetric measurements was later substantiated by XRD (Jamieson 1957; Davis 1964; Merrill and Bassett 1972, 1975; Bassett and Merrill 1973; Merrill 1974), Raman scattering (Fong and Nicol 1971; Nicol and Ellenson 1972; Liu and Mernagh 1990; Hess et al. 1991; Williems et al. 1992), ultrasonic (Wang 1968; Kondo et al. 1972; Vo Thanh and Lacam 1984), electrical resistance (Jamieson 1953), and volumetric (Singh and Kennedy 1974) measurements. These studies have shown that the calcite I $\rightarrow$ calcite II transition takes place at about 1.5 GPa. The transition from the rhombohedral ($R\bar{3}c$) to the monoclinic ($P2_1/c$) structure is of the displacive type with a density increase of about 2.2%, involving a rotation of the $CO_3^{-2}$ planar groups and a small displacement of the $Ca^{2+}$ cations (Hatch and Merrill 1981). The transition from calcite II to calcite III occurs at about 2.0 GPa. The structure of calcite II has been the subject of some controversy; a monoclinic structure (Merrill and Bassett 1972; Smyth and Ahrens 1997) and an orthorhombic structure (Davis 1964; Fiquet et al. 1994) have been suggested. In addition to calcite II and III, high-pressure and high-temperature phases labeled calcite IV and V have been found and these phases are commonly called disordered calcite, owing to the orientational disorder of the $CO_3^{-2}$ (Johansens and Puhan 1971; Cohen and Klement 1973; Reeder and Wend 1983; Dove and Powell 1989; Redfern et al. 1989; Fiquet et al. 1994).

Almost all previous experiments on the phase relations of $CaCO_3$ were limited to pressures below about 4 GPa. Recently $CaCO_3$ was shown to be useful as a catalyst/solvent for synthesis of diamond from graphite at about 8 GPa and above 2000 °C (Akaishi et al. 1990). Furthermore, with $CaCO_3$ as a catalyst, diamond crystals were grown on the faces of diamond seed crystals at 5.5 GPa and 1600~1800 °C (Kanda et al. 1991). Hence it is necessary to clarify the phase relations of $CaCO_3$ at pressures beyond 4 GPa to understand the mechanisms of the nucleation and growth involved in the diamond formation in the presence of $CaCO_3$.

In the present study, the phase relations of $CaCO_3$ have been studied at multiple $P$-$T$ points using various high-pressure techniques. These include synchrotron X-ray diffraction using a cubic anvil press, Raman scattering using a diamond-anvil cell, and post compression XRD on samples retrieved after heat treatment in an octahedral anvil press. The phase relations among calcite III, aragonite, disordered calcite (calcite IV, V), and liquid between 2 and 10 GPa and to 2000 °C have been delineated.

## EXPERIMENTAL METHODS

### Samples

Synthetic and natural calcite (i.e., calcite I) were used as starting materials. The synthetic sample was of reagent-grade

---

* E-mail: suito@mp.es.osaka-u.ac.jp

0003-004X/01/0009–997$05.00

(99.0% in purity), purchased from Wako Pure Chemical Industries, Ltd. The natural sample (99.95%) was a single crystal of calcite from Mexico. Powder XRD patterns of the two samples at ambient conditions showed that these samples were in a single crystalline phase of calcite I.

### High-pressure in situ experiments

High-pressure XRD measurements were carried out by using a cubic anvil type apparatus (MAX-90) installed at BL-14C of the Photon Factory, Institute of Materials Structure Science, High Energy Accelerator Research Organization (Shimomura et al. 1992). The apparatus carried six tungsten carbide anvils, each with a square top face of 6 mm edge length. Figure 1 shows a cross-sectional view of our cubic sample holder made of a mixture of amorphous boron and epoxy. The edge length of the cube was 8 mm. The sample was placed inside a graphite tube. Powdered NaCl used as a pressure marker was packed in a BN capsule and placed next to the sample. The pressure was estimated from the lattice parameter of NaCl based on the Decker equation of state (Decker 1971). High temperature was attained by passing a direct current through the graphite tube. The temperature was measured with a Pt-PtRh(13%) thermocouple that was inserted into the central part of the cube. No correction for the effect of pressure was made on the e.m.f. of the thermocouple.

Raman scattering measurements were undertaken up to 10 GPa at room temperature by using a gasketed diamond-anvil cell (Takemura et al. 1978). The gasket was made of a stainless steel with a 150 μm diameter hole drilled at the center. The natural single crystal was cut along a cleavage plane into a piece with dimensions of 80 × 80 × 20 μm. The sample and several tiny ruby crystals were mounted into the gasket hole together with a mixture of methanol, ethanol, and water in volume ratio of 16:3:1, which was used as a pressure transmitting medium. The pressure was measured by the ruby fluorescence method (Mao et al. 1978). The 514.5 nm line from an Ar ion laser was used for excitation and the laser beam was focused on the sample to a size of about 4 μm in diameter.

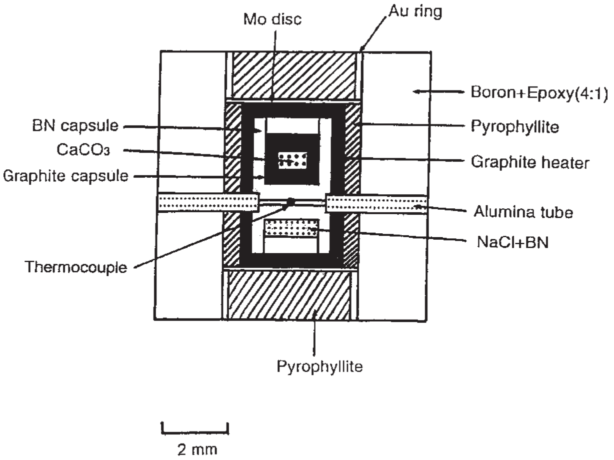

**FIGURE 1.** Cross-sectional view of a cubic sample cell for the in-situ X-ray diffraction experiment.

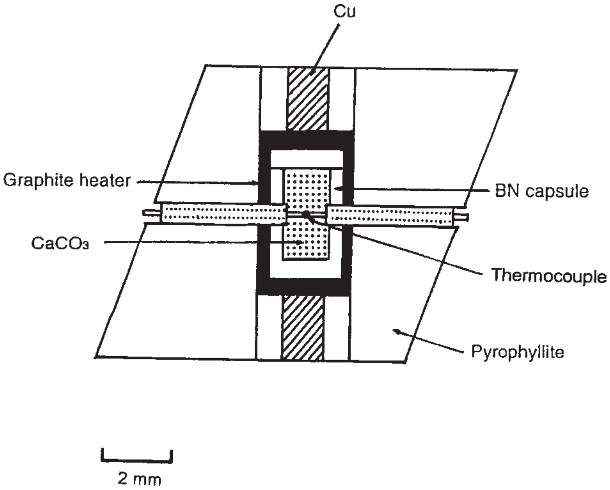

**FIGURE 2.** Cross-sectional view of an octahedral sample cell for the retrieval experiment.

### Retrieval experiment

In addition to in-situ high-pressure measurements, post-compression analyses by powder XRD were carried out on the samples after heat treatment in an octahedral anvil press (Onodera 1987). Pressure was calibrated at room temperature using the known pressure-induced phase transitions of Bi I-II(2.55 GPa), II-III(2.7 GPa), and III-V(7.7 GPa).

Figure 2 shows a cross-sectional view of the octahedral sample cell. The sample was packed in a capsule made of BN. A graphite tube was used for the heater. Duration of heating at a fixed pressure was normally 5 min. The temperature was measured by a Pt-PtRh(10%) thermocouple.

## RESULTS AND DISCUSSION

### In-situ study

Figure 3 shows XRD patterns of $CaCO_3$ recorded during the course of increasing pressure at room temperature. Although all of these patterns are similar, a detailed inspection reveals the occurrence of pressure-induced phase transitions. The pattern recorded at 0.49 GPa consists of calcite I only. At 1.70 GPa, a transition to calcite II occurs as indicated by appearance of the 013 line of calcite II and merging of the 204, 108, and 116 lines into a single broad peak. At 2.15 GPa, a small peak of the 002 calcite III line appears and becomes more pronounced at 2.94 GPa. The indexing of calcite III peaks in the 2.94 GPa pattern was made on the basis of an orthorhombic structure (Davis 1964). The cell constants of calcite III at 2.94 GPa were calculated to be $a = 8.55 \pm 0.04$ Å, $b = 8.34 \pm 0.04$ Å and $c = 7.11 \pm 0.03$ Å in agreement with the results of Davis (1964) and Fiquet et al. (1994). This series of experiments showed that the calcite III phase persists to at least 6.16 GPa at room temperature.

Figure 4 shows XRD patterns of $CaCO_3$ at four different temperatures at 6.16 GPa. Note that $CaCO_3$ is in the calcite III phase at 6.16 GPa at room temperature. Upon elevation of temperature, a transition from calcite III to aragonite occurs at 345

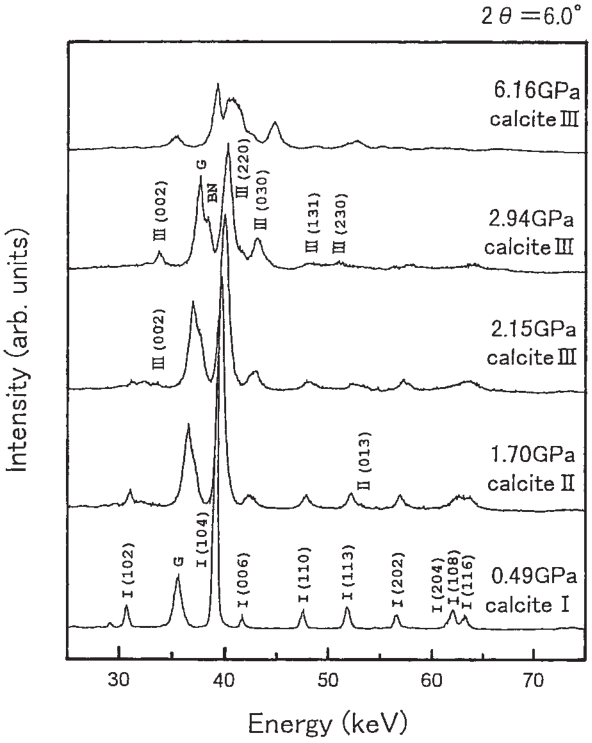

**FIGURE 3.** X-ray diffraction patterns of $CaCO_3$ at high pressure and at room temperature. The peaks labeled G and BN are from the heater and capsule, respectively (see Fig. 1)

°C, accompanied by a significant change in the diffraction pattern. A simple pattern with only three peaks is recorded at 1200 °C. This result shows that the aragonite phase transforms into another phase that is considered to be the same as calcite IV or V(disordered calcite). A further increase in temperature to 1730 °C causes these peaks to disappear, indicating that $CaCO_3$ is in the liquid phase.

Figure 5 shows XRD patterns after the liquefied $CaCO_3$ was rapidly cooled to room temperature. The bottom pattern in Figure 5, taken at 6.0 GPa and room temperature, is different from the pattern at the similar *P*-*T* condition before heating (see the bottom pattern in Fig. 4), but it is similar to that of aragonite. Upon release of pressure, the pattern became predominantly that of aragonite with a small amount of disordered calcite (the top pattern in Fig. 5). Thus, the sample retrieved from the liquid state to the ambient conditions is essentially aragonite. This feature helped monitor melting of $CaCO_3$ in the octahedral anvil-press experiments described later. The persistence of aragonite at ambient conditions can be ascribed to the negligible rate of the aragonite → calcite I transition at room temperature (Davis and Adams 1965). The present in-situ XRD study at ~ 6 GPa shows that calcite changes in the sequence: calcite III → aragonite → disordered calcite (calcite IV, V) → liquid as the temperature is raised. Such a sequence was also observed in a similar series of experiments carried out at 3 and 4 GPa.

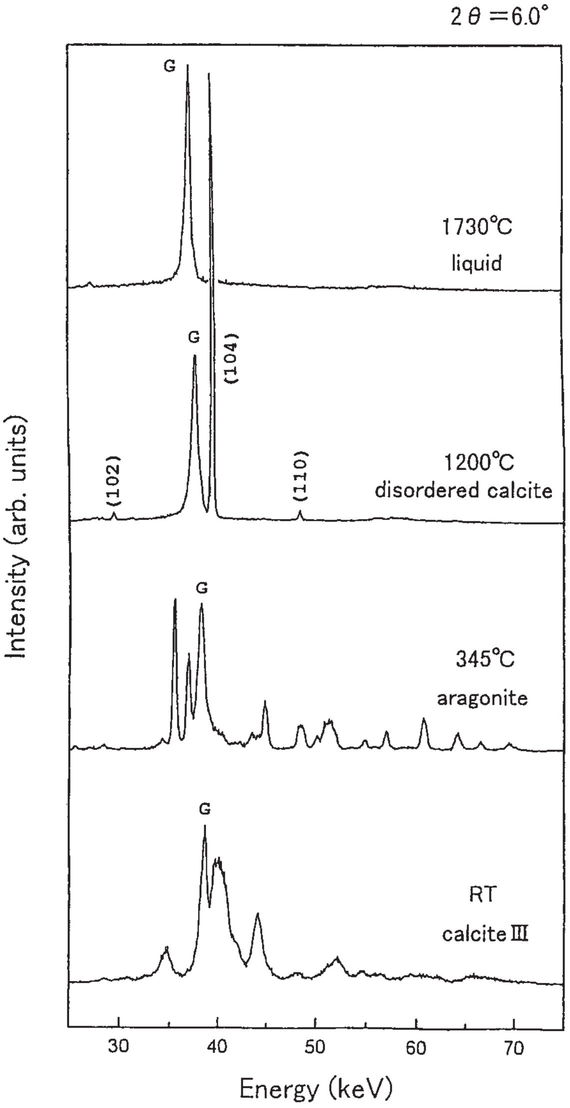

**FIGURE 4.** X-ray diffraction patterns of $CaCO_3$ during the course of heating at 6.16 GPa. The peak labeled G is from the heater (see Fig. 1).

Raman scattering spectra recorded at room temperature in the range 150 to 1600 $cm^{-1}$ are shown in Figure 6. The ambient-pressure spectrum shows five peaks assigned to one $A_{1g}$ mode (1083 $cm^{-1}$) and four $E_g$ modes (156, 282, 710, 1432 $cm^{-1}$), in agreement with previous reports (Nakagawa and Walter 1969; Fong and Nicol 1971; Nicol and Ellenson 1972; Liu and Mernagh 1990; Hess et al. 1991; Williems et al. 1992). At 1.7 GPa, a new peak (shown by the arrow) appears around 200 $cm^{-1}$, indicating a transition from calcite I to calcite II (Fong and Nicol 1971; Hess et al. 1991). A transition from calcite II to calcite III occurs at 1.90 GPa, as shown by the appearance of new peaks (shown by the daggers) at 280 $cm^{-1}$ and 1470 $cm^{-1}$ (Fong and Nicol 1971). These transition pressures for the calcite I → calcite II and calcite II → calcite III are in reasonable agreement with those probed by XRD (see Fig. 3). In the spectra recorded at 5.9 and 6.5 GPa, almost all the peaks characteristic of calcite III (Fong and Nicol 1971; Hess et al. 1991) appear. The spectrum at 10.0 GPa is somewhat different from the calcite III spectrum in that many small peaks appear in the 150–250 $cm^{-1}$ range, and instead, it becomes similar to that of aragonite taken at the same pressure (Kraft et al. 1991). The color of the crystal eventually changed to purple and it broke into several grains with a hexagonal shape. This behavior suggests a transition from calcite III to aragonite. However, because all of the peaks assigned to aragonite still appear at frequencies very near to those of calcite III, it is difficult to make a firm conclusion on the transition from calcite III to aragonite around 10 GPa.

## Retrieval study

Figure 7 shows XRD patterns of samples retrieved after heating to 1600 and 1750 °C at 5 GPa. The pattern from the 1600 °C treatment contains strong peaks of calcite I and a single, weak peak of aragonite, whereas that from 1750 °C consists simply of aragonite. Judging from the result of in-situ high-pressure XRD experiments described above, the pattern at 1750 °C indicates that the sample was liquefied at this temperature. Similar experiments at 4, 8, and 9 GPa, in combination with the in-situ XRD measurement, allowed us to determine the melting curve of $CaCO_3$.

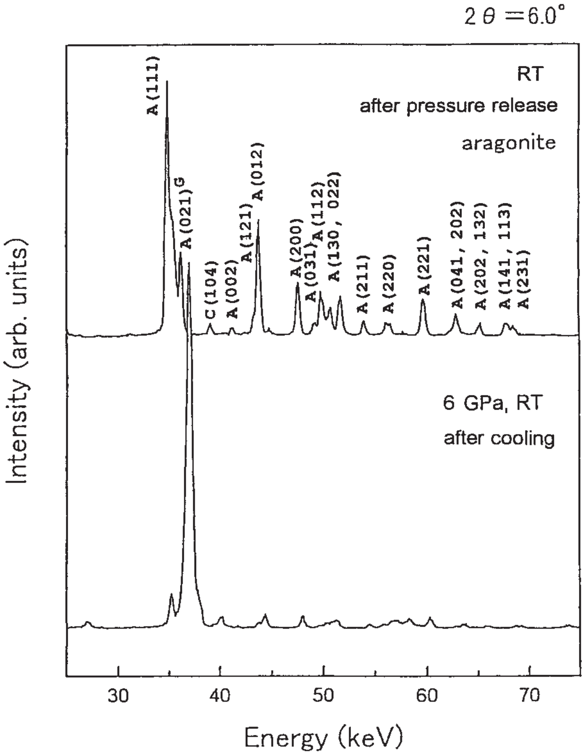

**FIGURE 5.** X-ray diffraction patterns taken after liquefied $CaCO_3$ was cooled. In the top pattern, G denotes the graphite heater, C the disordered calcite, and A the aragonite.

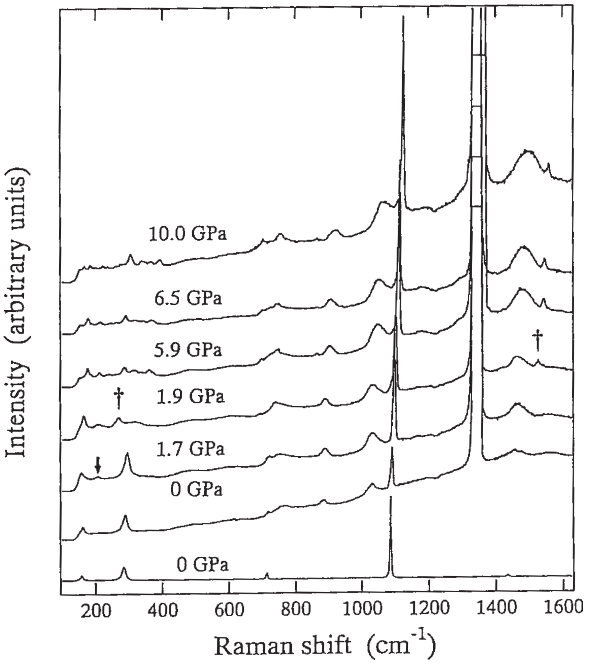

**FIGURE 6.** Raman spectra of $CaCO_3$ under ambient and high pressures at room temperature. The bottom spectrum was taken from the sample outside the diamond-anvil cell. Other spectra were recorded on the sample placed inside the diamond-anvil cell, showing diamond 1332 $cm^{-1}$ line from the anvil and some spurious peaks. (See text for explanation of the arrow and daggers.)

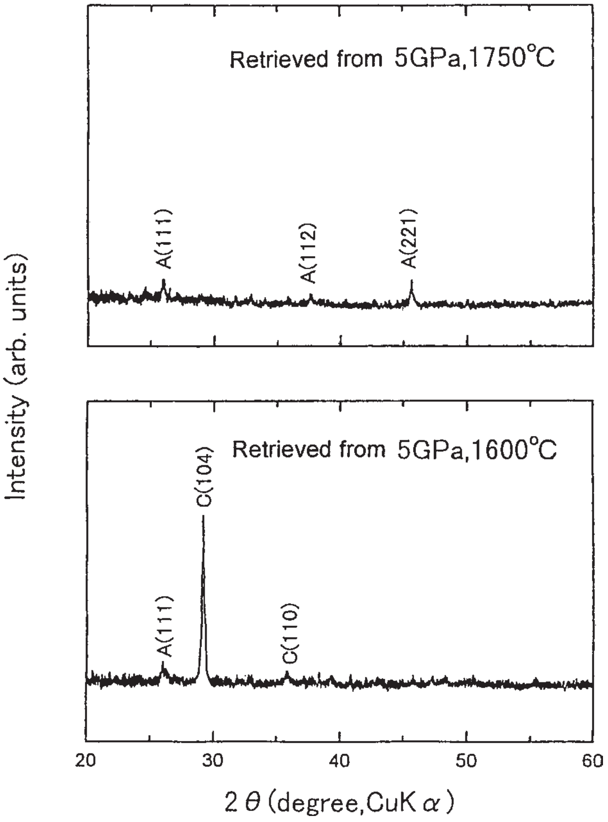

**FIGURE 7.** X-ray diffraction patterns of the samples retrieved from 5 GPa after heating to 1600 °C and 1750 °C. The letters C and A denote calcite and aragonite, respectively.

## Phase diagram

All of the data from the three categories of experiments performed in this work are displayed in Figure 8, which shows calcite I, II, and III, aragonite, disordered calcite (calcite IV, V), and liquid phases. The difference between calcite IV and V has not been determined in this study. The boundaries are obtained in most cases from heating processes at high pressures and hence do not necessarily represent thermodynamic equilibrium lines. The calcite III-aragonite boundary is bowed. It shows that the transition temperature increases with pressure from 2 to 4.5 GPa, above which the transition temperature decreases with increasing pressure. This should be compared with the study of Hess et al. (1991) who showed a negative slope for the calcite III-aragonite boundary in a range 1.8 ~ 3.9 GPa. The *P-T* phase boundary between aragonite and disordered calcite is linear with a slope of 125 °C/GPa. This boundary extrapolates to ambient pressure at 500 °C, which is about 480 °C lower than the transition temperature of calcite I to a high temperature phase of $CaCO_3$ (Mirwald 1976).

Most investigators have considered calcite II and III as metastable intermediary phases. Such a consideration arises from the fact that both calcite II and III appear within the stability field of aragonite (Merrill and Bassett 1975) and from a comparison of the densities of the two phases and aragonite. Smyth and Ahrens (1997) showed that both calcite II and III (based on the monoclinic structure) are less dense than aragonite, supporting the metastability of calcite II and III. On the other hand, Fiquet et al. (1994) reported that calcite III, when assigned to the orthorhombic structure, is denser than aragonite. The same assignment to the diffraction patterns in Figures 3 and 4 of the present study has revealed that the density of calcite III is higher than that of aragonite over wide ranges of *P-T* conditions: for example, 3.28 g/cm$^3$ at 2.94 GPa and room temperature and 3.48 g/cm$^3$ at 6.16 GPa and 170 °C in calcite III, compared with 3.05 g/cm$^3$ at 3 GPa and room temperature and 3.14 g/cm$^3$ at 6 GPa and 200 °C in aragonite (Martinez et al. 1996). Therefore, the comparison of the densities can work but requires a precise determination of the structure of calcite III.

Redfern et al. (1989) derived the phase boundary between calcite I and aragonite based on their calorimetric measurements along with considerations on the orientational disorder in calcite. The resultant boundary up to 2.6 GPa and 1200 K is curved, in agreement with the experiments. Calcite II and III appear right to this boundary, namely, in the stability field of aragonite.

In Figure 8 we have shown a negatively sloped boundary between calcite I and II based on the work of Bridgman (1938). Two other studies have shown a similar slope (Wang 1968; Kondo et al. 1972), but another study reported a positive slope for this boundary (Hess et al. 1991). The negative slope is more plausible from the Clausius-Clapeyron equation because the molar volume decreases across the calcite I → calcite II transition, and the entropy change is positive as the order parameter is lost owing to the soft-mode mechanism (Merrill 1974). Bridgman (1938) showed a positive slope for the boundary between calcite II and III, although the work of Hess et al. (1991) yielded a negative slope for this boundary.

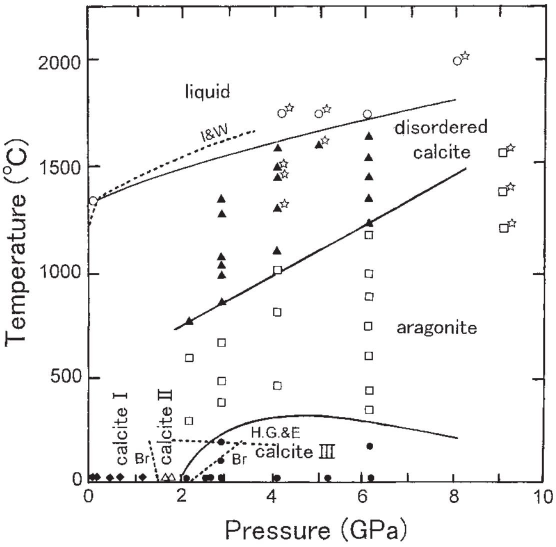

**FIGURE 8.** Phase relations of $CaCO_3$ obtained from the present experiments. Key: filled diamond = calcite I, open diamond = calcite II, filled circle = calcite III, open box = aragonite, open triangle = disordered calcite, open circle = liquid, □★, ○★, ▲★ = retrieval experiment, Br = After Bridgman (1938), H.G.& E = After Hess et al. (1991), I & W = After Irving and Wyllie (1975).

The curvature of the boundary between calcite III and aragonite (Fig. 8) can be interpreted in several ways. First, if it reflects a metastable calcite III → aragonite transition, the transition temperature could be governed by kinetics and might become lowered because of possible faster kinetics in the high-pressure regime. Second, the bowing may be attributed to a change in the order of transition from first to second as pressure is increased, as calcite III is likely to be a disordered or differently ordered variant of aragonite (Fong and Nicol 1971). Last, if we took the boundary between calcite III and aragonite as being mixed with the boundary between calcite II and III, it has a positive slope in the lower-pressure regime (Bridgman 1938) followed by a negative slope in the higher-pressure range (Hess et al. 1991) (namely, a combination of the two dotted lines Br and H.G.&E in Fig. 8, although the pressures where the two straight lines meet and the maximum of our boundary are a little different). Given the metastability of calcite III with respect to aragonite, the first interpretation appears to be feasible. However, as mentioned above, a question is raised as to the metastability. Point two has no thermodynamic basis at present. The third point can best explain the bowing of the calcite III-aragonite boundary and is supported by the experiments of Bridgman (1938) and Hess et al. (1991).

The melting point ($T_m$) of $CaCO_3$ is expressed as $T_m$ (°C) = 1338 + 82 $P$ – 2.9 $P^2$ ($P$ in GPa) up to 6 GPa. Irving and Wyllie (1975) reported the melting curve to 3.6 GPa from the texture of quenched samples. The two curves agree fairly well, although a deviation occurs with increasing pressure. An extrapolation of pressure to 8 GPa along our curve yields $T_m$ to be approximately 1800 °C, which is about 200 °C lower than the minimum temperature needed for the synthesis of diamond using $CaCO_3$ as a catalyst/solvent (Akaishi et al. 1990). Thus, the diamond formation should take place at temperatures higher than the melting point of $CaCO_3$ by about 200 °C. Below this temperature, the liquid $CaCO_3$ will not likely be an adequate catalyst/solvent for the formation of diamond. Similar behavior has been observed in some other oxygen-containing materials and inert materials as catalyst/solvent for diamond formation (Kanda 1994).

Figure 8 also suggests that the growth of diamond at 5.5 GPa and 1600 ~ 1800 °C (Kanda et al. 1991) can take place in the liquid state of $CaCO_3$ as $T_{\mathrm{m}} =$ 1700 °C at 5.5 GPa. It is not surprising that the growth temperature is significantly lower than that required for the synthesis at 8 GPa (Akaishi et al. 1990) because no nucleation is needed in this case. The melting point in this study suggests that the low-temperature regime of Akaishi et al.'s experiment could be in the solid state of $CaCO_3$. The development of catalytic activity in the solid phase has been noticed in some carbonized transition metals (Hosomi 1984; Perry et al. 1990). Although our study on the melting line of $CaCO_3$ has shed light on the formation of diamond in the presence of $CaCO_3$, further work is needed to determine other thermodynamic parameters in the carbon-$CaCO_3$ system, for example, the solubility and the eutectic temperature under pressure.

## ACKNOWLEDGMENTS

The authors are grateful to Francis H. Ree and Leo Merrill for reading and commenting on the manuscript. This work was carried out by approval of the Photon Factory Advisory Committee under no. 96 G 117.

## REFERENCES CITED

Akaishi, M., Kanda, H., and Yamaoka, S. (1990) Synthesis of diamond from graphite-carbonate systems under very high temperature and pressure. Journal of Crystal Growth, 104, 578–581.

Bassett, W.A. and Merrill, L. (1973) The crystal structure of $CaCO_3$(II), a metastable high-pressure phase of calcium carbonate. American Mineralogist, 58, 1106–1107.

Bridgman, P.W. (1938) The high pressure behavior of miscellaneous minerals. American Journal of Science, 237, 7–18.

Cohen, L.H. and Klement, Jr.W. (1973) Determination of high-temperature transition in calcite to 5 kbar by differential thermal analysis in hydrostatic apparatus. Journal of Geology, 81, 724–727.

Davis, B.L. (1964) X-ray diffraction data on two high pressure phases of calcium carbonate. Science, 145, 489–491.

Davis, B.L. and Adams, L.H. (1965) Kinetics of the calcite and aragonite transformation. Journal of Geophysical Research, 70, 433–441.

Decker, D.L. (1971) High pressure equation of state for NaCl, KCl and CsCl. Journal of Applied Physics, 42, 3239–3244

Dove, M.T. and Powell, B.M. (1989) Neutron diffraction study of tricritical orientational order/disorder phase transition in calcite at 1260 K. Physics and Chemistry of Minerals, 16, 503–507.

Fiquet, G., Euyot, F., and Itie, J-P. (1994) High-pressure X-ray diffraction study of carbonates: $MgCO_3$, $CaMg(CO_3)_2$ and $CaCO_3$. American Mineralogist, 79, 15–23.

Fong, M.Y. and Nicol, M. (1971) Raman spectrum of calcium carbonate at high pressures. Journal of Chemical Physics, 53, 579–585.

Hatch, D.H. and Merrill, L. (1981) Landau description of the calcite-$CaCO_3$ (II) phase transition. Physical Review B, 23, 368–374.

Hess, N. J., Ghose, S., and Exarhos, G.J. (1991) Raman spectroscopy at simultaneous high pressure and temperature: phase relations of $CaCO_3$ and the lattice dynamics of the calcite $CaCO_3$(II) phase transition. In A.K. Singh, Ed., Recent Trends in High Pressure Research; Proc. X IIIth AIRAPT International Conference on High Pressure Science and Technology, 236–241. Oxford & IBH Publishing Co. Pvt, Ltd., New Delhi.

Hosomi, S. (1984) Graphite-diamond conversion proceeded by the use of carburized cobalt solvent. Materials Research Bulletin, 19, 479–486.

Irving, A.J. and Wyllie, P.T. (1975) Subsolidus and melting relations for calcite, magnesite and joint $CaCO_3$-$MgCO_3$ to 36 kb. Geochimica et Cosmochimica Acta, 39, 36–53.

Jamieson, J.C. (1953) Phase equilibrium in the system calcite-aragonite. Journal of Chemical Physics, 21, 1385–1390.

———(1957) Introductory studies of high-pressure polymorphism to 24,000 bars by X-ray diffraction with some comments on calcite II. Journal of Geology, 65, 334–343.

Johansens, W. and Puhan, D. (1971) The Calcite-Aragonite transition, reinvestigated. Contributions to Mineralogy and Petrology, 31, 28–38.

Kanda, H., Akaishi, M., and Yamaoka, S. (1991) Morphology of synthetic diamond growth from carbonate solvent-catalysis. In R. Messier, Ed. New Diamond Science and Technology, p. 105–110, Materials Research Society International Conference Proceeding, Elesevier Science Publishing Co., Ltd., New York.

Kanda, H. (1994) Classification of the catalysis for diamond growth. In S. Saito, N. Fujimori, O. Fukunaga, M. Kamo, K. Kobashi, and M. Yoshikawa, Eds., Advances in New Diamond Science and Technology, p. 507–512, MYU Ltd., Tokyo.

Kraft, S., Knittle, E., and Williams, Q. (1991) Carbonate stability in the Earth's mantle: A vibrational spectroscopy study of aragonite and dolomite at high pressures and temperatures. Journal of Geophysical Research, 96, 17997–18009.

Kondo, S., Suito, K., and Matsushima, S. (1972) Ultrasonic observation of calcite I-II inversion to 700 °C. Journal of Physics of the Earth, 20, 245–250.

Liu, L.G. and Bassett, W.A. (1986) Elements, Oxides, and Silicate: High-Pressure Phases with Implications for the Earth's Interior. 134 p. Oxford University Press, New York.

Liu, L.G. and Mernagh, T.P. (1990) Phase transition and Raman spectra of calcite at high pressure and room temperature. American Mineralogist, 75, 801–806.

Mao, H.K., Bell, P.M., Shaner, J.W., and Steinberg, D.J. (1978) Specific volume measurements of Cu, Mo, Pd, and Ag and calibration of the ruby R1 fluorescence pressure gauge from 0.06 to 1 Mbar. Journal of Applied Physics, 49, 3276–3283.

Martinez, I., Zhang, J., and Reeder, R.J. (1996) In situ X-ray diffraction of aragonite and dolomite at high pressure and high temperature: evidence for dolomite breakdown to aragonite and magnesite. American Mineralogist, 81, 611–624.

Merrill, L. (1974) A soft mode mechanism for the displacive calcite -calcite (II) phase transformation at 1.5 GPa. In Proceedings of the 4th International Conference on High Pressure, Kyoto, p. 384–392, The Physico-Chemical Society of Japan.

Merrill, L. and Bassett, W.A. (1972) Crystal structure of the high-pressure phase of calcite. EOS Transactions, American Geophysical Union, 53, 1121.

———(1975) The crystal structure of $CaCO_3$(II), a high-pressure metastable phase of calcium carbonate. Acta Crystallographica, B31, 343–349.

Mirwald, P.W. (1976) A differential thermal analysis study of the high-temperature polymorphism of calcite at high pressure. Contributions to Mineralogy and Petrology, 59, 33–40.

Nakagawa, I. and Walter, J.L. (1969) Optical active crystal vibrations of the alkalic-metal nitrates. Journal of Chemical Physics, 51, 1389–1397.

Nicol, M. and Ellenson, W.D. (1972) Raman spectrum of $CaCO_3$ (III) at 77K. Journal of Chemical Physics, 56, 677–679.

Onodera, A. (1987) Octahedral-anvil high-pressure devices. High Temperatures-High Pressures, 19, 579–606.

Perry, J., Nelson, S., and Hosomi, S., (1990) Diamond formation in solid metal. Materials Research Bulletin, 25, 749–756.

Redfern, S.A.J., Salji, E., and Navtrotsky, A. (1989) High-temperature enthalpy at the orientational order/disorder transition in calcite: Implications of the calcite/aragonite phase equilibrium. Contributions to Mineralogy and Petrology, 101, 479–484.

Reeder, R.J. and Wend, H.R. (1983) Structure refinements of some thermally disordered dolomites. American Mineralogist, 68, 769–776.

Shimomura, O., Utsumi, W., Taniguchi, T., and Nagashima, T. (1992) A new high pressure and high temperature apparatus with sintered diamond anvils for synchrotron radiation use. In Y. Syono and M. Manghnani, Eds., High-pressure Research: Application to Earth and Planetary Sciences, Geophysical Monograph Series 67, p. 3–11. American Geophysical Union, Washington, D.C.

Singh, A.K. and Kennedy, G.C. (1974) Compression of calcite to 40 kbar. Journal of Geophysical Research, 79, 2615–2622.

Smyth, J.R. and Ahrens, T.J. (1997) The crystal structure of calcite (III). Geophysical Research Letters, 24, 1595–1598.

Takemura, K., Shimomura, O., Tsuji, K., and Minomura, S. (1978) Diamond-anvil pressure cell for x-ray diffraction studies with a solid-state detector. High Temperatures-High Pressures, 11, 311–316.

Vo Thanh, D. and Lacam, A. (1984) Experimental study of the elasticity of single crystalline calcite under high pressure (the calcite-calcite II transition at 14.6 kbar). Physics of the Earth and Planetary Interiors, 34, 195–203.

Wang, C. (1968) Ultrasonic study of phase transition in calcite to 20 kilobars and 180 °C. Journal of Geophysical Research, 73, 3937–3944.

Williems, Q., Collerson, B., and Knittle, E. (1992) Vibrational spectra of magnesite ($MgCO_3$) and calcite-III at high pressures. American Mineralogist, 77, 1158–1165.

MANUSCRIPT RECEIVED JUNE 8, 2000
MANUSCRIPT ACCEPTED MAY 1, 2001
MANUSCRIPT HANDLED BY JOHN RAKOVAN